Published in final edited form as:

Exp Eye Res. 2010 April ; 90(4): 493–500. doi:10.1016/j.exer.2009.12.012.

Role of Nrf2 in retinal vascular development and the vaso-obliterative phase of oxygen-induced retinopathy

Koichi Uno[a], **Tarl W. Prow**[a], **Imran A. Bhutto**[a], **Adi Yerrapureddy**[b], **D. Scott McLeod**[a], **Masayuki Yamamoto**[c], **Sekhar P. Reddy**[b], and **Gerard A. Lutty**[a,*]

[a]Wilmer Eye Institute, Johns Hopkins Hospital, Baltimore, MD, USA

[b]Johns Hopkins Bloomberg School of Public Health, Baltimore, MD, USA

[c]TARA, University of Tsukuba, Tsukuba, Japan

Abstract

In the initial stage of retinopathy of prematurity (ROP), hyperoxia causes retinal blood vessel obliteration. This is thought to occur in part through oxidative stress-induced apoptosis of endothelial cells. This study was designed to determine what role NF-E2-related factor 2 (Nrf2) plays in this process. Nrf2 is a transcription factor of the anti-oxidant response element that, if induced, may protect the retina from hyperoxia-induced oxidative stress. Nrf2 knockout mice (Nrf2−/−), Nrf2 wild type control mice (Nrf2 +/+), and C57BL/6 mice were exposed to hyperoxia (75% O_2) or normoxia from P7 through P12. Mice were sacrificed on P9 and P12 and the retinas were stained with GSA lectin-Cy3 to visualize retinal blood vessels. Hyperoxia exposed retinas were flat mounted and photographed, then the size of the avascular areas was determined. Additionally, retinas were cryopreserved after lectin staining and area analysis and then sectioned. Secondary or deep capillaries were then hand-counted in sections. In hyperoxia-treated mice, the avascular areas in Nrf2−/− P9 mice were significantly larger than those in Nrf2+/+ P9 mice ($P = 0.01$). However, there was no significant difference between Nrf2−/− and Nrf2+/+ mice at P12. Avascular areas at P12 were significantly smaller than that at P9 in Nrf2−/−, Nrf2+/+, and C57BL/6 mice ($P = 0.0011$, $P = 0.009$, and $P = 0.001$ respectively). The numbers of deep or secondary capillaries in air-reared Nrf2−/− mice were significantly decreased, when compared to Nrf2+/+ mice at P9 ($P = 0.0082$). On the other hand, there was no significant difference in deep capillary formation between air-reared Nrf2−/− and Nrf2+/+ mice at P12. Akt signaling activates Nrf2 and Akt was localized to retinal blood vessels in all animals and was increased in Nrf2+/+ and Nrf2−/− mice exposed to hyperoxia as compared to normoxia mice. Interestingly, during normal development this protection by Nrf2 occurs in a specific window of time that is also shared by angiogenesis. Hyperoxia treatment revealed a similar window of time where Nrf2 regulated anti-oxidant production was beneficial and contributed to the endothelial survival.

Keywords

blood vessels; development; hyperoxia; Nrf2; retinopathy of prematurity

*Corresponding author. Gerard A. Lutty, G. Edward and G. Britton Durell Professor of Ophthalmology, Wilmer Ophthalmological Institute, M041 Smith Building, 400 North Broadway, Johns Hopkins Hospital, Baltimore, MD 21287, USA. Tel.: +1 410 955 6750; fax: +1 410 955 3447. galutty@jhmi.edu (G.A. Lutty).

1. Introduction

Oxidative stress has been considered one of the leading causes of several ocular diseases, including age-related macular degeneration (AMD) (Ha et al., 2006; Kasahara et al., 2005), diabetic retinopathy (Kowluru et al., 2006a, 2006b), and retinopathy of prematurity (ROP) (Niesman et al., 1997). ROP is caused by exposure of a developing vasculature to hyperoxia, an oxidative insult. Developing retinal blood vessels in premature infants are particularly susceptible to increased oxygen levels. This is in contrast to adult retinal vasculatures, which are in fact not affected by hyperoxia other than being constricted (Gu et al., 2002; Patz, 1984). Premature infants are given supplemental oxygen in some cases after birth. The exposure to hyperoxia during this period causes developing retinal blood vessels to stop growing, constrict, and die. This is the vaso-oliterative phase of retinopathy of prematurity (ROP), which is one of the leading causes of blindness during childhood (Patz, 1954). ROP can be modeled in animals by exposing neonatal animals to hyperoxia which causes vaso-obliteration and death of endothelial cells, a model called oxygen-induced retinopathy (OIR) (McLeod et al., 1996a, 1998; Smith et al., 1994). It has been suggested that delivery of excess oxygen to the retina of neonates stimulates the generation of reactive oxygen species (ROS), which is thought to be responsible for the vaso-obliteration (Niesman et al., 1997).

Reactive oxygen species (ROS) are thought to be primarily generated by the mitochondria and result in oxidized proteins and lipids and, ultimately, damaged cells and tissues. Anti-oxidant enzymes like NAD(P)H: quinone oxidoreductase 1 (NQO1), glutathione S-transferases (GST), glutamate–cysteine ligase (GCL), and heme oxygenase 1 (HO-1) are constitutively expressed and function to reduce ROS. Recently, it has been shown that the expression of these enzymes can be regulated by a cis-acting regulatory element, the anti-oxidant responsive element (ARE)(Lee and Johnson, 2004). This system is regulated by an ARE-binding transcription factor called NF-E2-related factor 2 (Nrf2). Normally, Nrf2 resides in cytoplasm in an inactive state bound to Keap1. Exposure to various oxidants disrupts the Nrf2–Keap1 complex, leading to nuclear translocation of Nrf2 and the formation of a heterodimer with small Maf nuclear protein. This results in the transcriptional activation of ARE driven genes (Lee and Johnson, 2004; Srisook et al., 2005). Several studies revealed that hyperoxia induces severe damage to lung epithelial cells caused by ROS. Under hyperoxia-induced oxidative stress, the ARE was driven by Nrf2 transcription to protect lung epithelial cells from hyperoxic injury (Cho et al., 2002, 2005). Moreover, hyperoxia-stimulated Akt and ERK 1/2 kinase activation is critical for Nrf2-mediated transcription (Papaiahgari et al., 2004, 2006).

We hypothesize that ROS associated with hyperoxia may affect blood vessel development and result in vaso-obliteration. Therefore, the current study was designed to characterize the role of ARE transcription factor Nrf2 during retinal vascular development in normoxic or hyperoxic environments by using Nrf2+/+ and Nrf2−/− mice.

2. Materials and methods

2.1. Mice

Breeding pairs of ICR/CD1 Nrf2−/− mice and wild type background strain CD1 mice (Nrf2+/+) were obtained from a colony at Tsukuba University (Japan) and maintained in the Johns Hopkins Bloomberg School of Public Health (USA) (Itoh et al., 1997). Mice were fed a purified AIN-76A diet. Mice were bred, and progeny were genotyped as Nrf2+/+ or Nrf2−/−. C57BL/6 mice were obtained from Jackson Laboratory as mouse strain control. All experimental protocols conducted were performed in accordance with the ARVO Statement for the Use of Animals in Ophthalmic and Vision Research.

2.2. Oxygen exposure

Nrf2+/+, Nrf2−/−, and C57BL/6 mice were either exposed to room air or hyperoxia (75% oxygen) from postnatal day (P) 7 to P12. Mice were sacrificed at P9 and P12. After sacrifice, eyes were enucleated and then one eye was fixed in 2% paraformaldehyde overnight in Tris-buffered saline (TBS) at 4 °C for histopathological analysis described below. The retina from the fellow eye was harvested for mRNA analysis.

2.3. GSA-lectin staining

After fixation in 2% paraformaldehyde in Tris-buffered saline (TBS), anterior segments of the eyes were removed and then retinas were dissected from eyecups. Retinas were washed in TBS and then permeabilized with 1% Triton X in TBS. Retinas were incubated with biotinylated GSA-lectin (Sigma) in TBS (1:50 dilution) overnight at 4 °C. After washing 3 times with TBS, GSA lectin was labeled with Cy3-streptavidin in TBS (1:100 dilution) by overnight incubation at 4 °C. After staining, retinas were flat-mounted on glass slides and coverslipped. Flat-mount images were captured with a confocal microscope with 5× objective lens (Zeiss 510META). The area of the entire retina and the area of vaso-obliteration was determined from these images using Image J (http://rsb.info.nih.gov) and the percentage of retina with vaso-obliteration was determined from these measurements. Retinas were returned to Eppendorf tubes for cryopreservation after microscopy.

The retinas were then cryopreserved, embedded in OCT with 20% sucrose, and frozen for cryosectioning (Lutty et al., 1993). Eight micrometer cryosections were cut with a cryostat. Sections were briefly rinsed with TBS and then mounted with Prolong Gold (Invitrogen) mounting media containing Hoechst 33342. Pictures were taken with the Zeiss confocal microscope with 10× objective lens. Capillary counts (from inner to outer plexiform layer) were performed manually from the peripapillary region to the ora serrata.

2.4. Immunofluorescence

Cy3/GSA lectin-labeled cryosections were also used for immunofluorescence. Briefly, 8 μm-sections were fixed in absolute methanol for 5 min at –20 °C and then washed in PBS with 0.02% Triton X for 10 min. Sections were incubated for 60 min at room temperature with 2% normal goat serum in PBS with 0.02% Triton X. After washing with PBS, the sections were incubated with rabbit anti-Akt antibody (1: 200; Cell Signaling) in PBS with 0.02% Triton, overnight at 4 °C. After washing with PBS/0.02% Triton X, sections were

incubated with goat anti-Alexa Fluor 647 (Invitrogen) for 2 h at room temperature. Sections were washed with PBS with 0.02% Triton X, followed by mounting with Prolong Gold (Invitrogen). Digital images were collected using a Zeiss confocal microscope with 40× oil objective lens (Zeiss 510META). The number of deep capillaries was counted manually in these cross sections.

2.5. Real time PCR

After enucleation, retinas were dissected immediately and snap frozen with liquid nitrogen in an RNAse-free environment. RT-PCR was performed as previously published (Cho et al., 2002).

2.6. Statistical analysis

Unpaired two tail Student's *t*-test was used to compare the area of vaso-obliteration and the number of secondary capillaries between two groups. The P value <0.05 was considered significant.

3. Results

3.1. Vaso-obliteration in retina after oxygen exposure

Vaso-obliterated areas were quantified by image analysis (Fig. 1A–F) and the numerical results are shown Fig. 2. Vaso-obliteration in the retinas from Nrf2 knockout (Nrf2−/−) mice (Fig. 1B) was greater than that from wild type (Nrf2+/+) mice (Fig. 1A) at P9 ($P = 0.01$, Fig. 2). However, there was no significant difference in vaso-obliteration between Nrf2−/− retinas (Fig. 1E) and Nrf2+/+ retinas (Fig. 1D) at P12 (Fig. 2). In C57BL/6 mice (Fig. 1C and F), there was no significant difference in the area of vaso-obliteration compared to Nrf2−/− mice at P9. The area of vaso-obliteration in P12 retinas is smaller than that in P9 retinas in each group ($P < 0.01$, Figs. 1 and 2). GSA-lectin labeled retinas in each group showed that mostly retinal capillaries were absent in the hyperoxia-exposed mice, both at P9 and P12 (Fig. 1).

3.2. Development of retinal microvasculature

The development of the primary or superficial and secondary or deep vascular networks was examined by confocal microscopy. Examination of the retinas in cross sections demonstrated several similarities and some fundamental differences. The secondary network was reduced in Nrf2+/+ and C57Bl/6 hyperoxia-treated animals (Fig. 3) compared to air-reared animals (Fig. 4). In Nrf2−/− mice, there were no secondary or deep capillaries in hyperoxia (Fig. 3) or air control animals (Fig. 4). As mentioned above (Fig. 1), there was substantially less vaso-obliteration in the Nrf2+/+ mice as compared to Nrf2−/− mice.

Fundamental differences in the secondary network development of Nrf2+/+ and Nrf2−/− animals were identified under normoxic conditions. Although the primary retinal blood vessel net was forming at P9, there was a substantial decrease in the number of secondary capillaries in Nrf2−/− when compared to Nrf2+/+ retinas of the same age (Fig. 4). The number of secondary capillaries in Nrf2−/− retinas at P9 (Fig. 4) was significantly less than that in Nrf2+/+ retinas and C57BL/6 retinas at P9, when counted in cross sections (Fig. 5).

There was no significant difference in the number of secondary capillaries between Nrf2−/− retinas and Nrf2+/+ and C57BL/6 retinas at P12 suggesting that growth of this network rebounded from P9 (Fig. 5).

Superficial vasculature, including retinal arteries and veins, were formed at P9 in both Nrf2+/+ and Nrf2−/− retinas (Fig. 6A–D). However, more capillaries were present around veins in Nrf2−/− animals at both time points compared to Nrf2+/+ mice (Fig. 6, compare A–B to C–D). Secondary capillary network was forming at P9 (Fig. 6E) and completed at P12 (Fig. 6F) in the Nrf2+/+. Secondary capillaries were sparse at P9 in Nrf2−/− throughout the retinas when z-stacks of the inner retina were recorded from flat mounts. No obvious network was observed, only capillaries diving from the superficial network (Fig. 6G). The number of diving capillaries was increased in P12 Nrf2−/− retinas compared to the P9 Nrf2−/− (Fig. 6G and H) but the complete deep capillary network was not formed at either time point in Nrf2−/− mice.

3.3. Anti-Akt immunofluorescence and Akt mRNA expression in the developing vasculature

Akt immunohistochemistry primarily labeled retinal blood vessels, and the neural retina was only weakly stained. Retinal Akt expression was localized in superficial retinal blood vessels and deep capillaries in air control Nrf2 +/+ and Nrf2−/− animals at P9 (Fig. 7). Both Nrf2+/+ and Nrf2−/− P9 retinas show an obvious and similar increase in Akt immunostaining in superficial retinal blood vessels when the animals are exposed to oxygen for 2 days (Fig. 7). Anti-Akt immunofluorescence was increased in superficial retinal blood vessels and deep capillaries in P12 air control Nrf2−/−, when compared to Nrf2+/+ animals. Akt expression in retinal blood vessels was more prominent in both air-reared and oxygen-exposed Nrf2−/− animals at P12 compared to Nrf2+/+ mice (Fig. 8). At P9 the Akt mRNA decreased slightly in response to hyperoxic insult to 0.23 ± 0.01 and 0.15 ± 0.10 fold for Nrf2+/+ and Nrf2−/−, respectively, compared to Akt in normoxic Nrf2+/+ and Nrf2−/− retinas. RT-PCR confirmed that Akt mRNA was increased with hyperoxia in the P12 group. The P12 hyperoxia Nrf2+/+ animals showed a 1.49 ± 0.49 fold increase in Akt mRNA over the normoxic controls. The P12 Nrf2−/− animals also had increased Akt mRNA to 1.65 ± 0.50 fold increase compared to Nrf2+/+ animals. All RT-PCR data was normalized to β-actin mRNA levels.

4. Discussion

To date, the role of Nrf2 and the ARE in ocular development has not been described. Our study is the first investigation of Nrf2 in murine vascular development and its function as a protective element in ROS-induced ocular disease. The exact mechanisms contributing to the initial formation of the murine and human fetal retinal vasculatures are a matter of controversy. The human (McLeod et al., 2006) and canine (McLeod et al., 1987) superficial retinal vasculatures form from angioblasts in a process known as vasculogenesis. During this process angioblasts migrate and differentiate to assemble the initial fetal human retinal vasculature and dog neonatal retinal vasculature. In mouse, however, investigators have demonstrated that the retinal vasculature develops by angiogenesis (Fruttiger, 2002). Most

investigators agree that the deep or secondary vasculature in retina forms by angiogenesis in all species.

Whether the vasculature develops by angiogenesis or vasculogenesis, migration is required for development. Migration undoubtedly consumes energy and the process of differentiation requires adjustment to the proteome including degradation and expression. Therefore, the process of vasculature development is likely an energy consuming process. Increases in the production of ATP will ultimately increase oxidative stress (Videla, 2000). In addition, the murine photoreceptors develop inner segments and synapses at approximately P7 (Liu et al., 2006; Smith, 2002) and their phototransduction and excitation generates oxidative stress in retina (Dorfman et al., 2009). If this increase in oxidative stress is not met with an equal amount of cellular anti-oxidants, the normal developmental process may be altered. Nrf2 is one of the major proteins that regulates anti-oxidant gene expression. By removing this major player in the Nrf2−/− mice, we expected to gain insight into the role of anti-oxidants during vascular development. Hyperoxia-induced mRNA levels of NQO1, GST, UDP glycosyl transferase (UGT), glutathione peroxidase-2 (GP×2), and HO-1 were significantly lower in lungs of Nrf2−/− mice compared to Nrf2+/+ mice (Cho et al., 2002). However, one complication in interpretation is that, although Nrf2 is a major factor in expression of antioxidants, there are other signaling pathways that regulate the anti-oxidant response (Cho et al., 2002).

The secondary capillary network in the retina appears to form by angiogenesis in most species (Fruttiger, 2002; Hughes et al., 2000; McLeod et al., 1996b, 1987). Interestingly, this was the developmental process most dramatically affected by loss of Nrf2 (Figs. 3–6). Those results suggest that there are some fundamental developmental differences between the formation of the primary and secondary networks. One possibility is that the angiogenic process occurring in the secondary network formation generates increased levels of oxidative stress. In this same area in retina, newly formed photoreceptor inner segment mitochondria (Smith, 2002) may be generating oxidative stress as well. In addition, the increased metabolic demands of differentiation and migration may make the endothelial cells in the deep network more susceptible to the oxidative insult generated by the photoreceptor visual transduction system. Our data shows that the lag observed in secondary network development in Nrf2−/− animals at P-9 approaches normal levels by P12. One logical hypothesis is that the lack of sufficient anti-oxidants leads to a slowing of the angiogenic process initially but, by P-12, the endothelial cells have somehow compensated for the loss of Nrf2 and angiogenesis has rebounded to normal levels. This compensation may be due to increased VEGF production in areas with inadequate deep capillaries. Stone et al. suggested that Muller cells make VEGF during deep capillary development (Stone et al., 1995). It is interesting that all three strains of mice had rebound from vaso-obliteration at P12 even though hyperoxia was still present, so mouse may have a compensatory anti-oxidant mechanism that does not depend on Nrf2 for activation.

With increased oxygen, however, there was increased vaso-obliteration in the P9 Nrf2−/− mice, with respect to the wild type (Nrf2+/+) controls implies that the endothelial cells of the Nrf2-deficient animals underwent additional oxidative stress, which caused additional vaso-obliteration compared to Nrf2+/+ animals. However, this was only true at P9. At P12

there were no significant differences between the Nrf2−/− and the Nrf2+/+ suggesting that the retinal vasculature can recover from the initial hyperoxic insult, even in the absence of Nrf2. The cause of vaso-obliteration has been a matter of controversy for some time, but ROS is one of the most likely components. Others have suggested that peroxidation is the key to vaso-obliteration in oxygen-induced retinopathy (Brooks et al., 2001; Hardy et al., 2000). Perhaps photoreceptor activity induces expression of anti-oxidants secreted by RPE, Muller cells or astrocytes. We have previously shown that hyperoxia inhibits several processes critical to both vasculogenesis and angiogenesis that may not be ROS related (Uno et al., 2007). Admittedly this work was done with an in vitro model, but the data may have some implications for the current study. One is the possibility that increased oxygen may cause signaling disruptions that lead to vaso-obliteration. This could result in a number of effects ranging from the obvious, apoptosis, to some more creative alternatives like dedifferentiation of endothelial cells (Uno et al., 2007). Ultimately, more investigation into the mechanisms of oxygen-induced retinopathy needs to be done to answer these questions.

One of the major signaling components of the ARE system is Akt (Papaiahgari et al., 2006). The complex Akt signaling pathway is thought to promote cell survival. Therefore, we utilized immunofluorescence and RT-PCR to elucidate Akt localization and mRNA levels in this model. The limited Akt data reported herein is not intended to establish causality, but to set the stage for future investigations into signaling mechanisms at work in OIR. The obvious localization of relatively high levels of Akt in blood vessels shown in Figs. 7 and 8 suggest functionality in both normal development and in OIR. The RT-PCR data correlates with the immunofluorescence observations at P12, but not P9. The regulation of Akt during OIR appears to be a complex series of events that needs to be fully investigated with quantitative protein and mRNA studies and immunolocalization of phospho-Akt, which were unable to accomplish due to our inability to find a reliable antibody for mouse phospho-Akt. Additionally, other signaling pathways may well contribute to vaso-obliteration (Papaiahgari et al., 2006).

In summary, the present study demonstrated that Nrf2−/− mice are more susceptible to increased vaso-obliteration compared to Nrf2+/+ mice when they were exposed to hyperoxia for 2 days. These data indicate that Nrf2 protects retinal vascular cells from oxidative stress caused by hyperoxia. Retinal vascular development, especially formation of retinal secondary capillary network, was delayed as well in Nrf2−/− mice at P9 after air exposure so Nrf2 may play a role in normal vascular development. Akt, the main intracellular signaling pathway for blood vessel growth, expression was observed in retinal blood vessels in both Nrf2−/− and Nrf2+/+ mice. Akt expression was increased when the animals were exposed in hyperoxia for 2 days. Finally, Nrf2 appears not to be the only pathway for activation of anti-oxidant enzymes in retina because both vaso-obliteration during hyperoxia and normal development of the deep capillary system approached normal by P12 in Nrf2−/− mice.

Acknowledgments

This work was supported by National Eye Institute grant R01EY09357 (GL), EY 01765 (Wilmer), and the Johns Hopkins Hematology Training grant T32HL007525 (TP) and NIH grant HL66109 (SPR). Gerard Lutty received an RPB Senior Investigator Award in 2008.

References

Brooks SE, Gu X, Samuel S, Marcus DM, Bartoli M, Huang PL, Caldwell RB. Reduced severity of oxygen-induced retinopathy in eNOS-deficient mice. Invest Ophthalmol Vis Sci. 2001; 42:222–228. [PubMed: 11133872]

Cho HY, Jedlicka AE, Reddy SP, Kensler TW, Yamamoto M, Zhang LY, Kleeberger SR. Role of NRF2 in protection against hyperoxic lung injury in mice. Am J Respir Cell Mol Biol. 2002; 26:175–182. [PubMed: 11804867]

Cho HY, Reddy SP, Debiase A, Yamamoto M, Kleeberger SR. Gene expression profiling of NRF2-mediated protection against oxidative injury. Free Radic Biol Med. 2005; 38:325–343. [PubMed: 15629862]

Dorfman AL, Joly S, Hardy P, Chemtob S, Lachapelle P. The effect of oxygen and light on the structure and function of the neonatal rat retina. Doc Ophthalmol. 2009; 118:37–54. [PubMed: 18483821]

Fruttiger M. Development of the mouse retinal vasculature: angiogenesis versus vasculogenesis. Invest Ophthalmol Vis Sci. 2002; 43:522–527. [PubMed: 11818400]

Gu X, Samuel S, El-Shabrawey M, Caldwell RB, Bartoli M, Marcus DM, Brooks SE. Effects of sustained hyperoxia on revascularization in experimental retinopathy of prematurity. Invest Ophthalmol Vis Sci. 2002; 43:496–502. [PubMed: 11818396]

Ha KN, Chen Y, Cai J, Sternberg P Jr. Increased glutathione synthesis through an ARE-Nrf2-dependent pathway by zinc in the RPE: implication for protection against oxidative stress. Invest Ophthalmol Vis Sci. 2006; 47:2709–2715. [PubMed: 16723490]

Hardy P, Dumont I, Bhattacharya M, Hou X, Lachapelle P, Varma DR, Chemtob S. Oxidants, nitric oxide and prostanoids in the developing ocular vasculature: a basis for ischemic retinopathy. Cardiovasc Res. 2000; 47:489–509. [PubMed: 10963722]

Hughes S, Yang H, Chan-Ling T. Vascularization of the human fetal retina: roles of vasculogenesis and angiogenesis. Invest Ophthalmol Vis Sci. 2000; 41:1217–1228. [PubMed: 10752963]

Itoh K, Chiba T, Takahashi S, Ishii T, Igarashi K, Katoh Y, Oyake T, Hayashi N, Satoh K, Hatayama I, Yamamoto M, Nabeshima Y. An Nrf2/small Maf heterodimer mediates the induction of phase II detoxifying enzyme genes through antioxidant response elements. Biochem Biophys Res Commun. 1997; 236:313–322. [PubMed: 9240432]

Kasahara E, Lin LR, Ho YS, Reddy VN. SOD2 protects against oxidation-induced apoptosis in mouse retinal pigment epithelium: implications for age-related macular degeneration. Invest Ophthalmol Vis Sci. 2005; 46:3426–3434. [PubMed: 16123448]

Kowluru RA, Atasi L, Ho YS. Role of mitochondrial superoxide dismutase in the development of diabetic retinopathy. Invest Ophthalmol Vis Sci. 2006a; 47:1594–1599. [PubMed: 16565397]

Kowluru RA, Kowluru V, Xiong Y, Ho YS. Overexpression of mitochondrial superoxide dismutase in mice protects the retina from diabetes-induced oxidative stress. Free Radic Biol Med. 2006b; 41:1191–1196. [PubMed: 17015165]

Lee JM, Johnson JA. An important role of Nrf2-ARE pathway in the cellular defense mechanism. J Biochem Mol Biol. 2004; 37:139–143. [PubMed: 15469687]

Liu J, Wang J, Huang Q, Higdon J, Magdaleno S, Curran T, Zuo J. Gene expression profiles of mouse retinas during the second and third postnatal weeks. Brain Res. 2006; 1098:113–125. [PubMed: 16777074]

Lutty GA, Merges C, Threlkeld AB, Crone S, McLeod DS. Heterogeneity in localization of isoforms of TGF-b in human retina, vitreous, and choroid. Invest Ophthalmol Vis Sci. 1993; 34:477–487. [PubMed: 7680639]

McLeod DS, Brownstein R, Lutty GA. Vaso-obliteration in the canine model of oxygen-induced retinopathy. Invest Ophthalmol Vis Sci. 1996a; 37:300–311. [PubMed: 8603834]

McLeod DS, Crone SN, Lutty GA. Vasoproliferation in the neonatal dog model of oxygen-induced retinopathy. Invest Ophthalmol Vis Sci. 1996b; 37:1322–1333. [PubMed: 8641835]

McLeod DS, D'Anna SA, Lutty GA. Clinical and histopathologic features of canine oxygen-induced proliferative retinopathy. Invest Ophthalmol Vis Sci. 1998; 39:1918–1932. [PubMed: 9727415]

McLeod DS, Hasegawa T, Prow T, Merges C, Lutty G. The initial fetal human retinal vasculature develops by vasculogenesis. Dev Dyn. 2006; 235:3336–3347. [PubMed: 17061263]

McLeod DS, Lutty GA, Wajer SD, Flower RW. Visualization of a developing vasculature. Microvasc Res. 1987; 33:257–269. [PubMed: 2438539]

Niesman MR, Johnson KA, Penn JS. Therapeutic effect of lipsomal superoxide dismutase in an animal model of retinopathy of prematurity. Neurochem Res. 1997; 22:597–605. [PubMed: 9131639]

Papaiahgari S, Kleeberger SR, Cho HY, Kalvakolanu DV, Reddy SP. NADPH oxidase and ERK signaling regulates hyperoxia-induced Nrf2-ARE transcriptional response in pulmonary epithelial cells. J Biol Chem. 2004; 279:42302–42312. [PubMed: 15292179]

Papaiahgari S, Zhang Q, Kleeberger SR, Cho HY, Reddy SP. Hyperoxia stimulates an Nrf2-ARE transcriptional response via ROS-EGFR-PI3K-Akt/ERK MAP kinase signaling in pulmonary epithelial cells. Antioxid Redox Signal. 2006; 8:43–52. [PubMed: 16487036]

Patz A. Clinical and experimental studies on role of oxygen in retrolental fibroplasia. Trans Am Acad Ophthalmol Otolaryngol. 1954; 58:45–50. [PubMed: 13146729]

Patz A. Current concepts of the effect of oxygen on the developing retina. Curr Eye Res. 1984; 3:159–163. [PubMed: 6197238]

Smith LEH, Wesolowski E, McLellan A, Kostyk SK, D'Amato RD, Sullivan R, D'Amore PA. Oxygen-induced retinopathy in the mouse. Invest Ophthalmol Vis Sci. 1994; 35:101–111. [PubMed: 7507904]

Smith, RS. Systemic Evaluation of the Mouse Eye: Anatomy, Pathology, and Biomethods. CRC Press; Washigton, D.C: 2002.

Srisook K, Kim C, Cha YN. Molecular mechanisms involved in enhancing HO-1 expression: de-repression by heme and activation by Nrf2, the “one–two” punch. Antioxid Redox Signal. 2005; 7:1674–1687. [PubMed: 16356129]

Stone J, Itin A, Alon T, Pe'er J, Gnessin H, Chan-Ling T, Keshet E. Development of retinal vasculature is mediated by hypoxia-induced vascular endothelial growth factor (VEGF) expression by neuroglia. J Neurosci. 1995; 15:4738–4747. [PubMed: 7623107]

Uno K, Merges CA, Grebe R, Lutty GA, Prow TW. Hyperoxia inhibits several critical aspects of vascular development. Dev Dyn. 2007; 236:981–990. [PubMed: 17366630]

Videla LA. Energy metabolism, thyroid calorigenesis, and oxidative stress: functional and cytotoxic consequences. Redox Rep. 2000; 5:265–275. [PubMed: 11145101]

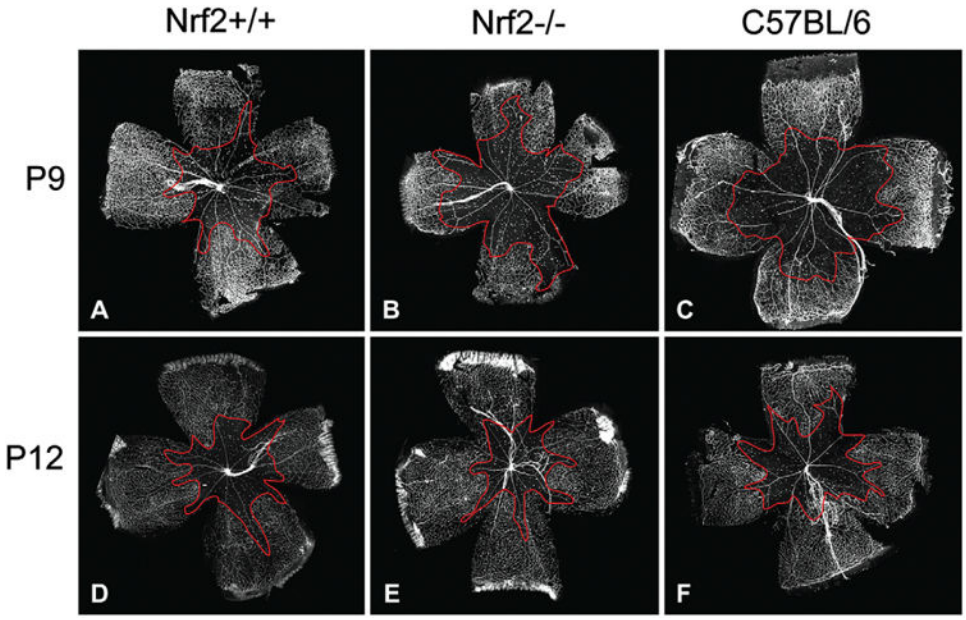

Fig. 1.

Vaso-obliterated areas are outlined in red in P9 and P12 retinas from Nrf2+/+, Nrf2−/−, and C57BL/6 animals treated with hyperoxia. These representative lectin-stained retinas show the gross differences in the areas of vaso-obliteration between the three groups of mice.

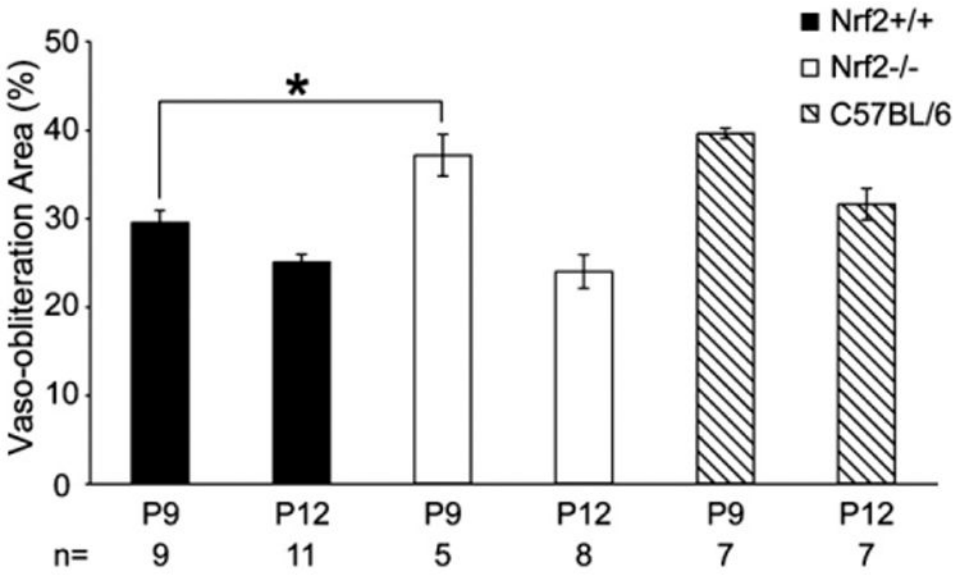

Fig. 2.

The percentage of retina with vaso-obliteration in the lectin-stained retinas after two (P9) and five days (P12) of hyperoxia. The mean percent area of retina with vaso-obliteration in each group was compared between Nrf1−/− and Nrf1+/+ mice at each time point by unpaired *t*-test. Asterisk indicates $P < 0.05$ between Nrf+/+ and Nrf−/− mice at P9 and the bars indicate SEM.

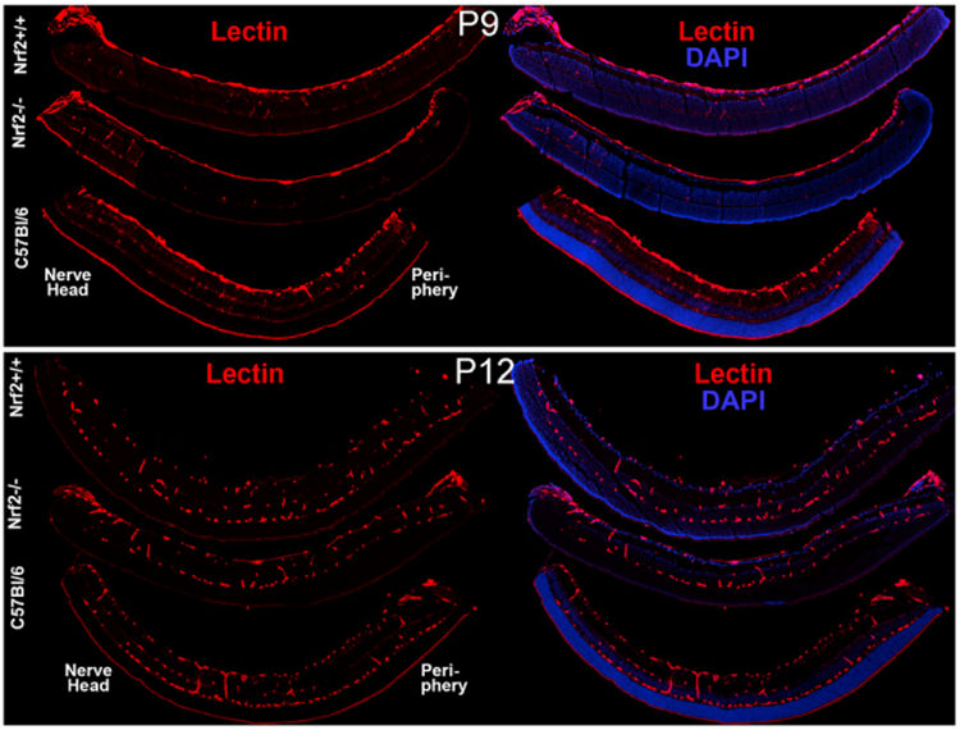

Fig. 3.

Lectin (red) labeled sections in each hyperoxia-treated group were photographed to illustrate the presence of retinal capillaries. Retinal nuclei were counterstained by Hoechst 33342 (blue). Orientation of retinas is noted as nerve head and periphery.

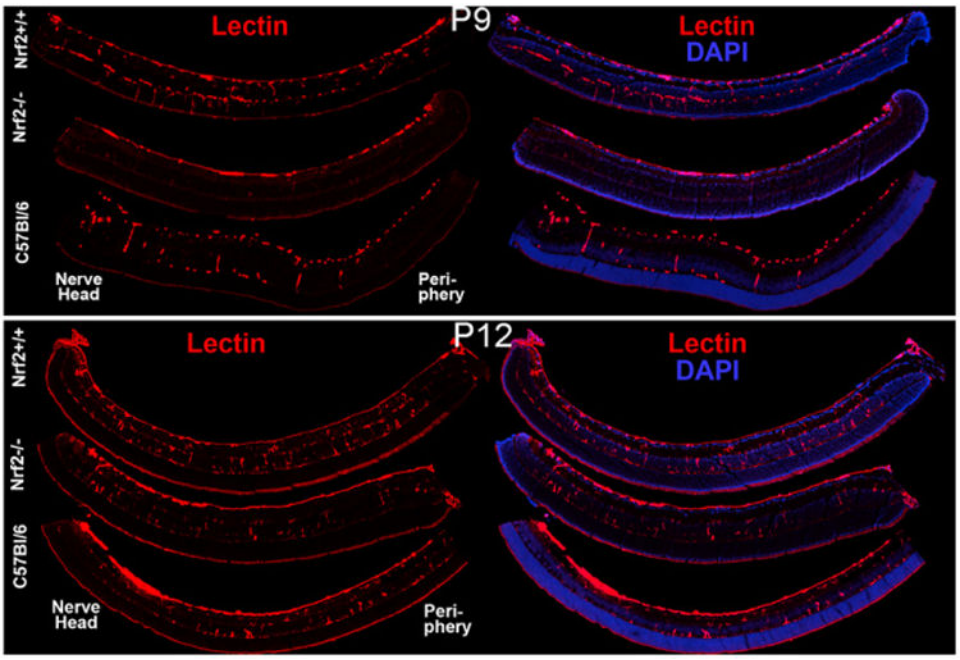

Fig. 4.

Lectin (red) labeled sections in each air control group were photographed to illustrate the presence of retinal capillaries. Retinal nuclei were counterstained with Hoechst 33342 (blue).

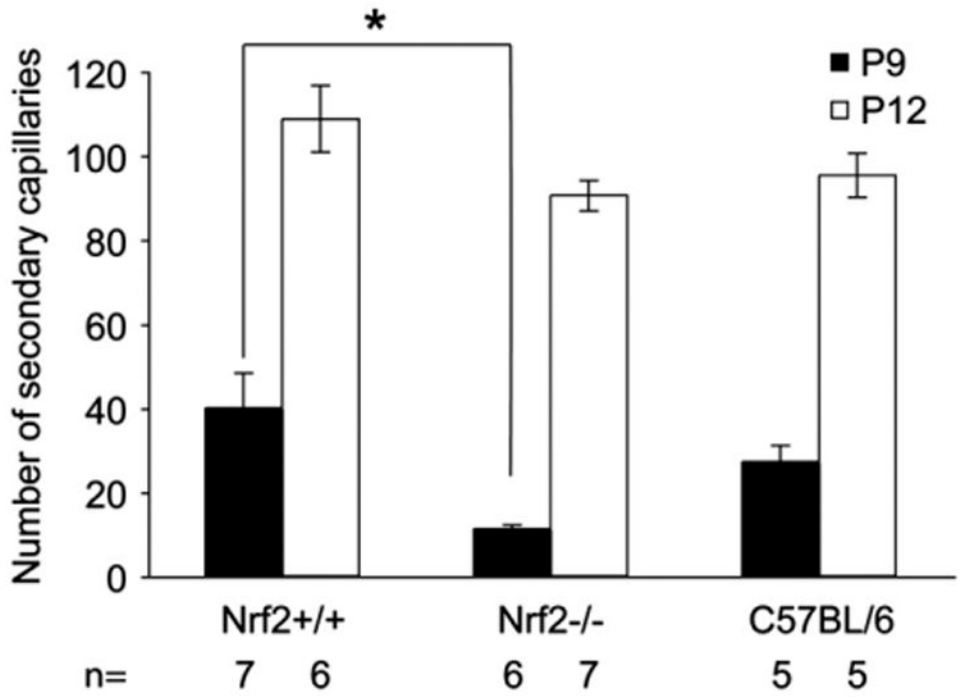

Fig. 5.

The number of secondary or deep capillaries per section in air control animals was determined by hand counts from images like those shown in Fig. 4. The number of secondary capillaries was compared between Nrf1−/− and Nrf1 +/+ mice and analysed by an unpaired *t*-test Asterisk indicates a significant difference ($P < 0.05$) between Nrf2+/+ and Nrf2−/− mice and between Nrf2−/− mice and C57BL/6 control groups at P9. There was a significant difference in number of secondary capillaries between P9 and P12 animals in all three groups, which is not indicated ($P < 0.01$). The bars indicate SEM.

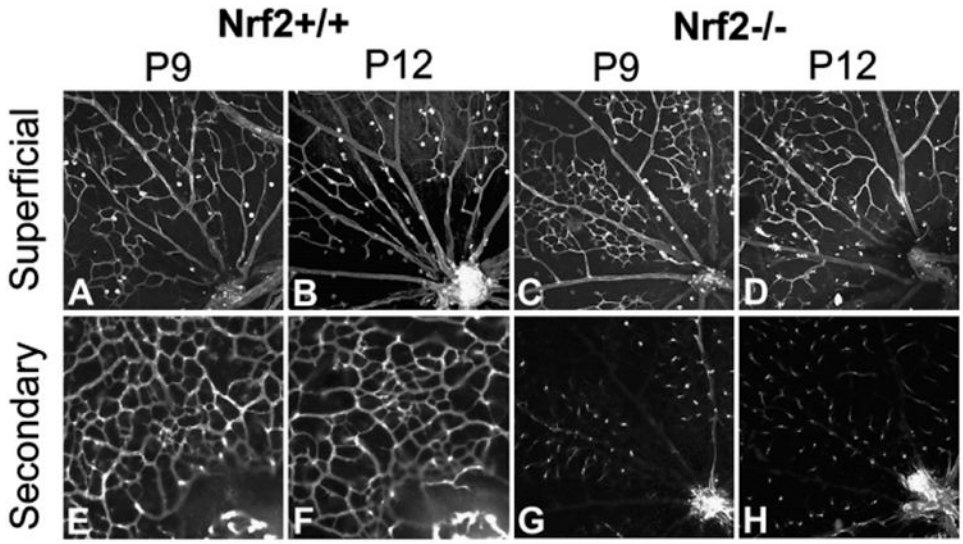

Fig. 6.

Optical slices from Z-stacks of the superficial vasculature and the secondary capillary network were captured in Lectin-stained flat mounts from air-treated animal retinas by confocal microscopy.

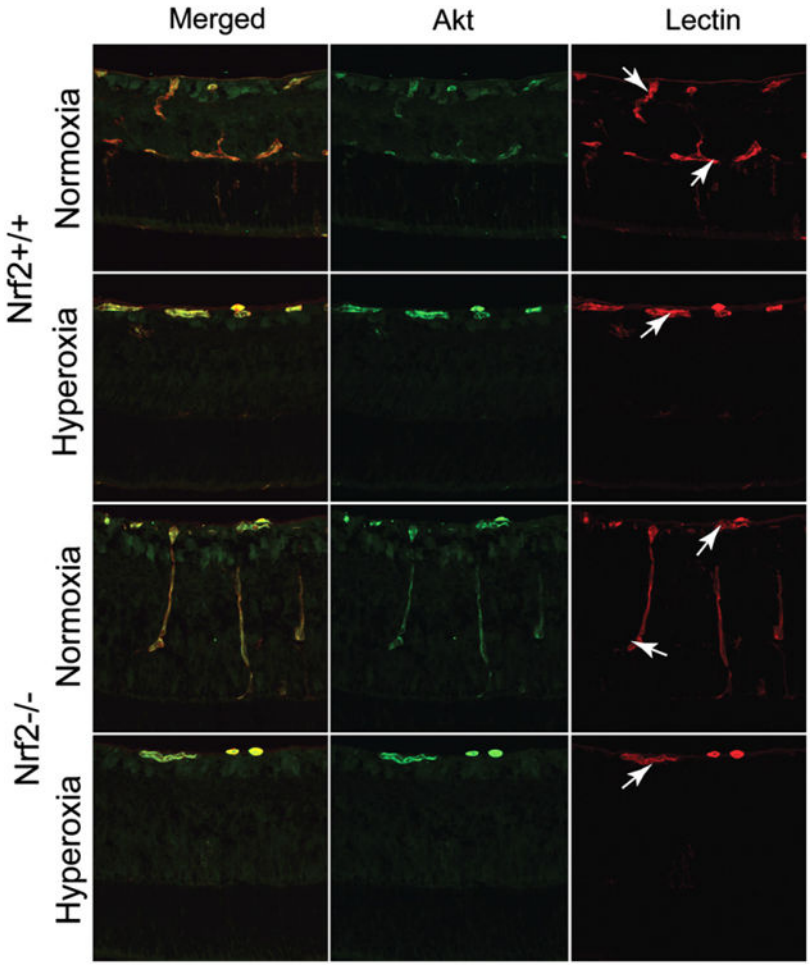

Fig. 7.

Anti-Akt immunofluorescence (green) in cross-sections of P9 retinas reared in normoxia and hyperoxia. Akt is almost exclusively associated with retinal blood vessels (red, lectin labeled).

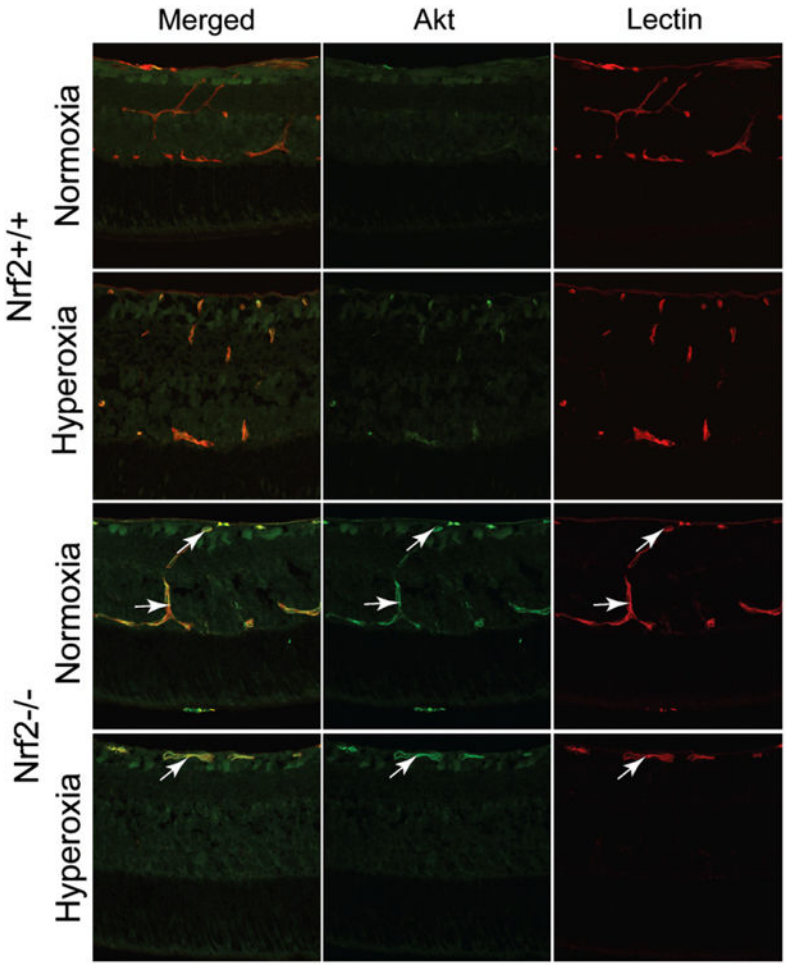

Fig. 8.

Akt labeling (green) in cross-sections of P12 retinas reared in normoxia and hyperoxia. Retinal blood vessels were labeled with the lectin (red).